5D.4 IMPACT OF STABLE BOUNDARY LAYER ON TROPICAL CYCLONE STRUCTURE AND INTENSITY ON COUPLED WRF MODEL

Chiaying Lee*

RSMAS/University of Miami

1. INTRODUCTION

It has been recognized that air-sea interaction plays an important role in Tropical Cyclones (TCs) intensity. A recent study by Lee and Chen (2012) showed that a persistent cold wake can have a significant impact on the hurricane boundary layer (HBL) structure, and introduces an asymmetry in HBL. However, the physical mechanism for connecting this asymmetrically distributed ocean feature with TCs structure through the HBL and the moist convective processes in TCs is still missing.

Recent observations from the Impact of Typhoons on the Ocean in the Pacific (ITOP) have shown that storm-induced ocean cooling can lead to development of a persistent stable boundary layer (SBL) in TCs (see section 11B.1). To fully understand the physical processes of stable boundary layer over the cold wake in TCs and its impact on storm structure, a comprehensive tracer and trajectory analysis is conducted using the coupled WRF-3DPWP (CWRF) model simulation of Typhoon Choiwan (2009). Experiments of uncoupled WRF and CWRF are compared to quantify the thermodynamic and dynamic properties of the inflow air over the storm-induced cold wake/SBL. It is found that the near surface inflow air in the stable boundary layer in CWRF tends to stay in BL longer, penetrate further inward into the TC inner core and eyewall with higher equivalent potential temperature due to an enhanced surface heat fluxes, whereas more of the air in an unstable and/or neutral boundary layer in the WRF tends to go into rainbands, and less amount into the TC inner core.

The ratio of the mass-weighted kinetic energy change and air-sea enthalpy flux in Choiwan shows that CWRF is about 16% more efficient than WRF at the period when both storm reaches quasi-steady state and there is a persistent cold wake in CWRF. These results suggest that the cold wake and stable boundary layer partially mitigate the direct weakening effect of the cold wake, and increase the efficiency of a mature storm.

2. COUPLED MODEL AND THE IMPLEMENTATION OF TRACER AND TRACJECTORY

2.1 CWRF

CWRF is composed of WRFV3.1.1 and 3DPWP. In WRF, WSM5 is used as the microphysical scheme and YSU is used as the boundary layer scheme with wind-depend surface roughness based on Donelan (2004). The modified thermal exchange coefficient over water based on Garratt's (1992) parameterization is used, too. 3DPWP is a multi-layer upper ocean model that contains three-dimensional physical processes: vertical mixing, horizontal advection, vertical advection, and pressure gradient. It vertically extends to 390 m, which is deep enough for hurricane simulation purpose.

* *Corresponding Author:* Chia-Ying Lee, University of Miami, Email: clee@rsmas.miami.edu

2.2 Forward Lagrangian Tracer and trajectory

A Lagrangian trajectory is a single air-particle that is integrated forward with time, following the airflow, and only advection is considered. One important characteristic of the trajectory is that it is an undiluted air-parcel. By using a passive tracer, Romps and Kuang (2010) found that the undiluted updrafts are negligible above height of 4-5 km, indicating the importance of mixing processes. Additionally, the mixing processes in TCs are essential since the development and the maintenance of the vortex relies on the mixing of air between the vortex, BL, and the environment. Hence, to complete our analyses, a tracer, an air-parcel that is subjected to not only advection but also mixing and diffusion, is also used in this study. We embed the trajectory calculation into CWRF, and therefore each trajectory particle is integrated forward every time step through the WRF dynamic core. The tracer calculation was originally one of the WRF-chemistry package (WRF-CHEM). With collaboration of NCAR scientist, we are able to modify WRF and use it as one of the scalar variables. The biggest advantage of our implementation is the improved accuracy, which can avoid all the potential error when using a low frequent model.

In this study, we released tracer and trajectories over the cold wake region in CWRF, and in the same storm relative location in WRF.

3. SUPER-TYPHOON CHOIWAN

3.1 Track and intensity forecast

Overall CWRF and WRF have a very similar evolution of track and intensity (Fig. 1). They are both influenced by the subtropical ridge and move along its edge. They quickly intensify on the 13th, and become mature storms at the beginning of the 14th. Then, they stop strengthening for about 18 hours. WRF started to rapidly intensify again and reaches its peak intensity late on the 15th while CWRF peaks near the beginning of the16th. They are both at quasi steady state early on the16th and start to weaken later on. Over the whole forecast period, the near identical tracks of WRF and CWRF provide a favorable condition for the comparison. Therefore, the differences of storm intensity and structure can be assumed to solely response to the air-sea interaction, i.e. the integral effect of ocean coupling in CWRF. During the whole forecast period, we choose first 12 hours on 16 Sep. as our periods of interest, after both storm reached their peak intensity and are in a quasi-steady state in this period.

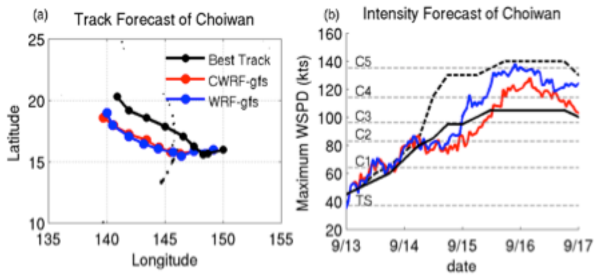

Figure 1: (a) The model forest tracks from CWRF (red) and WRF (blue) along with the JMA (solid black) and JTWC (dashed-black) best track data.

3.2 Convective structures

By analyze the radar reflectivity field at 1 km altitude (Fig. 2), we found that there appears to be some resemblance in eyewall and rainband structures between these two simulations. The similarities include the symmetric eyewall, the radius of maximum wind speed (RMW, ~35 km), the location of the primary rainband, and the persistent outer rainband southeast of the storm. However, the convection over the cold wake and at downwind area adjacent to the cold wake is weaker in CWRF than in WRF, which could be a consequence of the non-local effect of the cold wake induced stabilized inflow which will be further discussed in the next paragraph.

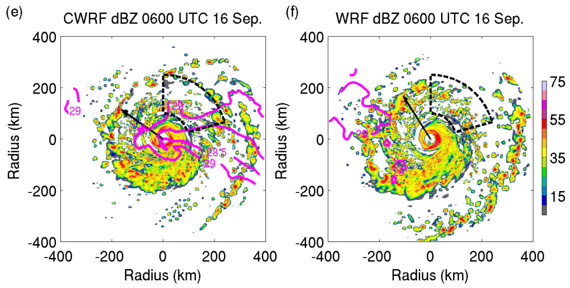

Figure 2: The simulated radar reflectivity at 1 km altitude in CWRF (left) and WRF (right) with SST

3.3 SBL in CWRF

To examine the exact location of the SBL and its relation to the storm induced cold wake, we calculated the stability of surface layer and of HBL. Within this whole period, the strongest cooling is about 2.5 ^{o}C. The stable surface layer covers almost the whole cold wake area outside of the primary rainband. The SBL is inside of stable surface layer area and covers a smaller region. This implies that the SBL is a result of the time and spatially integrated influence of cold wake, and the cold wake stabilizes the surface first before vertically stabilizes the whole BL. One more point is that there is no SBL underneath strong convective zone, such as eyewall and primary rainband, and this might be due to the mixing processes caused by convection.

4. THE IMPACT IF STABLE BOUNDARY LAYER ON NEAR SURFACE INFLOW

4.1 The evolution of near surface inflow

A comprehensive analysis of tracer and trajectory calculation shows that the over the cold wake, the near surface flow in CWRF has a tendency staying in BL longer and being further inward transported into the eyewall (Fig.3). However, without the impact of the stable BL, the near-surface flow over the same storm relative location tends to be vertically transported into the convective rainband instead of going into the eyewall. As a result, there is higher tracer concentration the eyewall.

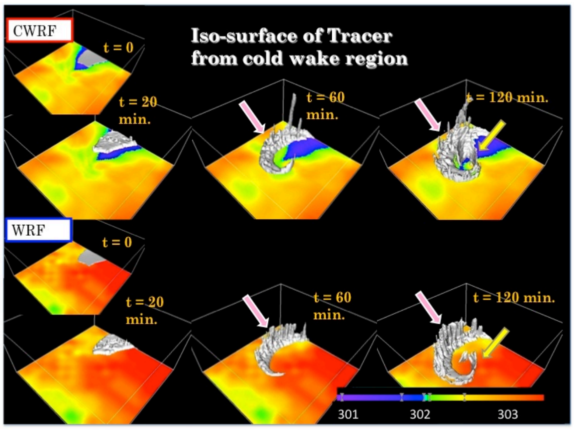

Figure 3: The iso-surface (gray) of the cold-wake tracer in CWRF (top panels) and WRF (bottom panels) at 0, 20, 60, 120 minutes after it is released. The color shading indicates the SST. The pink arrows point to the tracer that is vertically transported into the outer rainband while the yellow arrows point to that entering the eyewall.

4.2 Dynamic and thermodynamic inflow

The airflow is driven by either dynamic forcing or thermodynamic forcing, or both of them. Here we try to separate the cause of the different behaviors of the near surface inflow between CWRF and WRF into these two factors. The results from analyzing convective structure have implied that the thermodynamic impact of the SBL could be the suppressed convective activities (Fig. 2). This explains why there is higher tracer concentration in BL in CWRF than WRF but not why there is the further inward eyewall penetration of tracer from cold wake in CWRF. By comparing the inflow strength and inflow angle over the whole storm and over the cold wake area, we found that there is an apparent further inward turning of near inflow in CWRF when the airflow start to entering the cold wake area (Fig. 4). The forming of this dynamic effect could be the sudden change of turbulent mixing and BL height as argued in Chen et al. (2010), or the potential forming of inertial BL (personal communication with Dr. Ralph Foster, 2010), or the change of local pressure gradient due to the SST gradient.

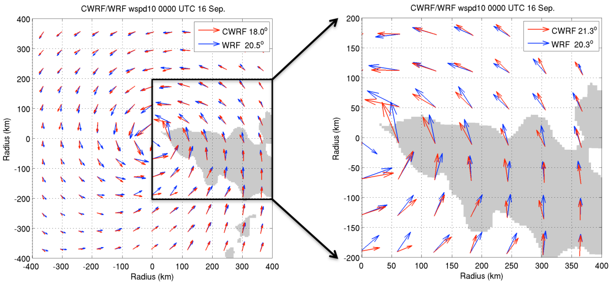

Figure 4: The 10-meter wind vectors for CWRF (red) and WRF (blue) at 0000 UTC 16 September. The gray shading shows the 1 °C SST cooling and the storm motion is roughly to west-northwest (black line). The cold wake and it adjacent downstream area is enlarged at the right.

4.3 Energetic impact and storm efficiency

A TC can be viewed as a heat engine converting heat energy extracted from the ocean into the kinetic energy (KE) through the diabetic heating in moist convection. The efficiency of converting thermal energy into KE in a storm is therefore defined as a ratio between the change of mass-weighted KE (δKE) and the mass-weighted surface enthalpy fluxes (EFLX) within a control volume. The control volume is defined as a cylinder with the lateral boundary at 350 km from a storm center and then is vertically integrated over the whole model. Then, CWRF efficiency is normalized by the WRF one. If this value is larger than one, CWRF is more efficient than WRF and vise versa

We calculated the storm efficiency over a 6-hours period from 00z to 06 on both 15th and 16th Sep. to present the difference between the intensification period and the steady state period. For the intensification period, the ratio of CWRF efficiency to WRF is 0.66, i.e., the storm in CWRF is 34% less efficient then WRF, which is associated with storm intensity. At the quasi-steady state, CWRF has induced a significant cold wake, and is weaker than WRF. However WRF has efficiency of 0.028 while CWRF has it of 0.032, which means that a weak storm in CWRF is 14% more efficient than a strong storm in WRF. Comparing the inner-core δKE to the whole 350-km vortex δKE, it is apparent that the rainband convection contributes to the increase of KE in WRF at quasi-steady state since the inner-core δKE decreases. However, the increase of KE in CWRF comes from both the eyewall and rainband convection.

5. CONCLUSION

In this study, we discuss an important issue about how the storm-induced cold wake changes the BL characteristics and then the convective structure energetically and eventually increase the storm efficiency. In summary, a new mechanism in CWRF is found: the stabilized BL over the cold wake alters the inflow properties. Thermodynamically, it results in air-parcel staying in the BL longer, and gaining more energy. Dynamically, it enhances the surface inflow angle, which results in more ari-parcel penetrating into the eyewall. The combination consequence of the dynamic and thermodynamic impacts is that there is more high-energy air entering the eyewall, increasing the storm efficiency. It is argued that while the direct negative feedback caused by SST cooling dominates, the stabilizing effect of the cold wake can oppose and partially mitigate this negative feedback.

6. REFERENCE

Chen, S., Tim J. Campbell, Hao Jin, Saša Gaberšek, Richard M. Hodur, Paul Martin, 2010: Effect of Two-Way Air–Sea Coupling in High and Low Wind Speed Regimes. Mon. Wea. Rev., 138, 3579–3602

Lee, C.-Y. and S. S. Chen, 2012: Symmetric and asymmetric structures of hurricane boundary layer in coupled models and observations, J. Atmos. Sci,(in review).

Romps, David M., Zhiming Kuang, 2010: Do Undiluted Convective Plumes Exist in the Upper Tropical Troposphere?. J. Atmos. Sci., 67, 468–484.